Computers and Mathematics with Applications 64 (2012) 822–832

Contents lists available at SciVerse ScienceDirect

Computers and Mathematics with Applications

journal homepage: www.elsevier.com/locate/camwa

Maximum power point tracking and optimal Li-ion battery charging control for photovoltaic charging system

Her-Terng Yau, Qin-Cheng Liang, Chin-Tsung Hsieh *

Department of Electrical Engineering, National Chin-Yi University of Technology, Taichung 411, Taiwan

ARTICLE INFO

Keywords:
Photovoltaic (PV)
Variable Step Size Incremental Conductance method
Genetic algorithms (GA)

ABSTRACT

Due to the severity of the global energy crisis and environmental pollution, the photovoltaic (PV) system has become one kind of important renewable energy source. Solar energy has the advantages of maximum reserve, inexhaustibleness, and is free from geographical restrictions, thus making PV technology a popular research topic. This study is aimed at developing a PV charging system for Li-ion batteries by integrating Maximum Power Point Tracking (MPPT) and charging control for the battery. In order to enable the solar cell to use the sunlight effectively, a DC/DC boost converter for solar power generation was first designed, which used the MPPT Algorithm of Variable Step Size Incremental Conductance Method (INC) to enable the solar cell to track the MPPT at any time. The output from the DC/DC boost converter then entered the DC/DC buck converter to reduce the voltage for charging purposes. The charging system uses a constant voltage method to charge the Li-ion battery. The PI controller design Constant Voltage (CV) charging method uses a genetic algorithm to determine the optimal gain value. The numerical simulation showed that the PV charging system proposed by this study is easily realized, and can resist the disturbance of external environmental changes, and achieve fast charging.

1. Introduction

The photovoltaic (PV) system has developed rapidly in the past decade, and has become a mature technology. It is considered an important renewable energy as it is a clean energy that is easy to maintain and produces very low noise. However, as it can use sunlight for only a limited time within a day, and also depends on the weather and environmental conditions, the PV system must have a Maximum Power Point Tracking (MPPT) controller to enable the system to utilize solar energy most efficiently at any time [1].

At present, the common MPPT control methods include: (1) voltage feedback method, which obtains the voltage of MPPT of solar cell in a fixed environment; although its design is simple, this method cannot track the MPPT in different climatic environments automatically [2]; (2) perturbation and observation method (P&O), which increases or decreases the terminal voltage of the solar cell in a fixed duty cycle; if the perturbation causes the output power of the solar cell to rise, the perturbation will keep moving in the same direction, so as to increase the voltage of the solar cell; on the contrary, if the perturbation causes the output power of the solar cell to decrease, the perturbation will move in the inverse direction, so as to reduce the voltage of the solar cell to track the MPPT; its defect is that there will be an oscillation effect when the operation reaches the MPPT, so the electrical energy cannot be utilized effectively [3]; (3) incremental conductance method (INC), which searches for $dP/dV = 0$, based on a similar control principle as P&O; when its step is large, its tracking speed will be high, but the steady-state oscillation amplitude will also be large; on the contrary, when its step is small, the

* Corresponding author.
E-mail address: fred@ncut.edu.tw (C.-T. Hsieh).

0898-1221/$ – see front matter © 2012 Elsevier Ltd. All rights reserved.
doi:10.1016/j.camwa.2011.12.048

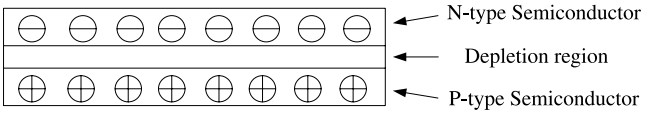

Fig. 1. Schematic diagram of solar cell.

tracking will be slow, and the steady-state oscillation will be reduced relatively [4]. This study is discussed the INC, and uses the Variable Step Size Incremental Conductance Method to realize the MPPT of the solar cell [5].

Under the development of portable equipment, the secondary Li-ion battery has become the electrical energy source for most portable products, such as mobile phones, notebook computers, and PDAs. At present, the common Li-ion battery charging control methods include: (1) Constant Voltage charging method (CV): this method controls the voltage of a fully charged battery at the set voltage, so the battery will not be over charged; (2) Constant Current charging method (CC): under normal conditions, when the Li-ion battery is fully charged, its temperature does not change excessively, and the CC compares the normally working temperature change as the cut-off condition; this charging method is inapplicable to a Li-ion battery [6]; (3) Constant Current/Constant Voltage charging method (CC/CV), this method is two-stage charging, the battery is charged at a constant current at the first stage, when the battery voltage reaches the set value, it is charged at a constant voltage [7,8]; (4) Pulse charging method: this method uses a recurrent pulse current to charge the battery, the battery has a rest period when charging in order to prolong the battery life [9]; (5) Reflex charging method: this method is similar to the pulse charging method, and based on the pulse charging method, the discharge pulse current is supplied during pulse current charging in order to extend the battery life [10]. Among the above methods, the CC is inapplicable to the Li-ion battery; the design of the CC/CV, pulse charging method and reflex charging method is complicated and inapplicable to the design of small solar cell chargers. Therefore, this study used the CV method, which has a simple structure, with the control circuit easily realized on portable devices, so as to save cost.

Based on the PV technology, this study integrated a PV system with a Li-ion battery charging system [11], combined with the Variable Step Size Incremental Conductance Method, and used CV at the battery end to control the charging of the Li-ion battery. The PI controller of CV used genetic algorithms (GA) to determine the optimal K_P and K_I values, so as to realize fast charging of the Li-ion battery.

2. Characteristics of a solar cell

A solar cell combines the PV semiconductor, P-type semiconductor and N-type semiconductor for solar power generation. It generates electron holes and electrons when it is irradiated by sunlight, so the current flows through to generate power. The principle of photovoltaic power generation is shown in Fig. 1.

Whether the solar cell is in series or parallel connection, its mathematical model can be simply expressed as

$$I_{PV} = I_{ph} - I_{sat}\left(\exp\frac{q}{BkT}V_{PV} - 1\right) \tag{1}$$

where

I_{PV}: Output current (A) of solar cell,	V_{PV}: output voltage (V) of solar cell,
I_{sat}: Reverse saturation current of solar cell,	I_{ph}: Current generated by solar cell,
q: Quantity of electronic charge,	k: Boltzmann constant,
B: Ideal factor of solar cell,	T: Solar cell surface absolute temperature.

The power–voltage and current–voltage curves of a solar cell in standard test conditions (i.e. 1000 W/m^2 solar irradiance, AM1.5, 25°) corresponding to a mathematical model are shown in Fig. 2.

3. MPPT system design

The step of the MPPT Algorithm of traditional INC is fixed. If the large step control is adopted, the solar cell can track the MPPT rapidly; however, the large step tracking also causes a larger oscillation effect in the steady-state, thus resulting in low efficiency output. On the contrary, if the MPPT is tracked slowly, the oscillation is small in the steady-state. Therefore, the step fixed INC must select either instantaneousness or steady-state.

This study used the Variable Step Size Incremental Conductance Method [12], which can track the MPPT rapidly. As the steady-state oscillation is very slight, its efficiency is better than that of traditional INC.

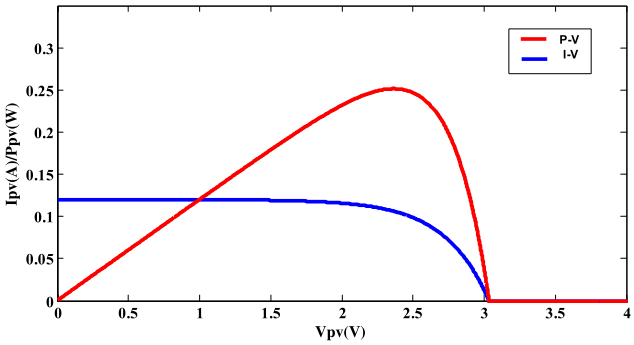

Fig. 2. Characteristic curves of solar cell.

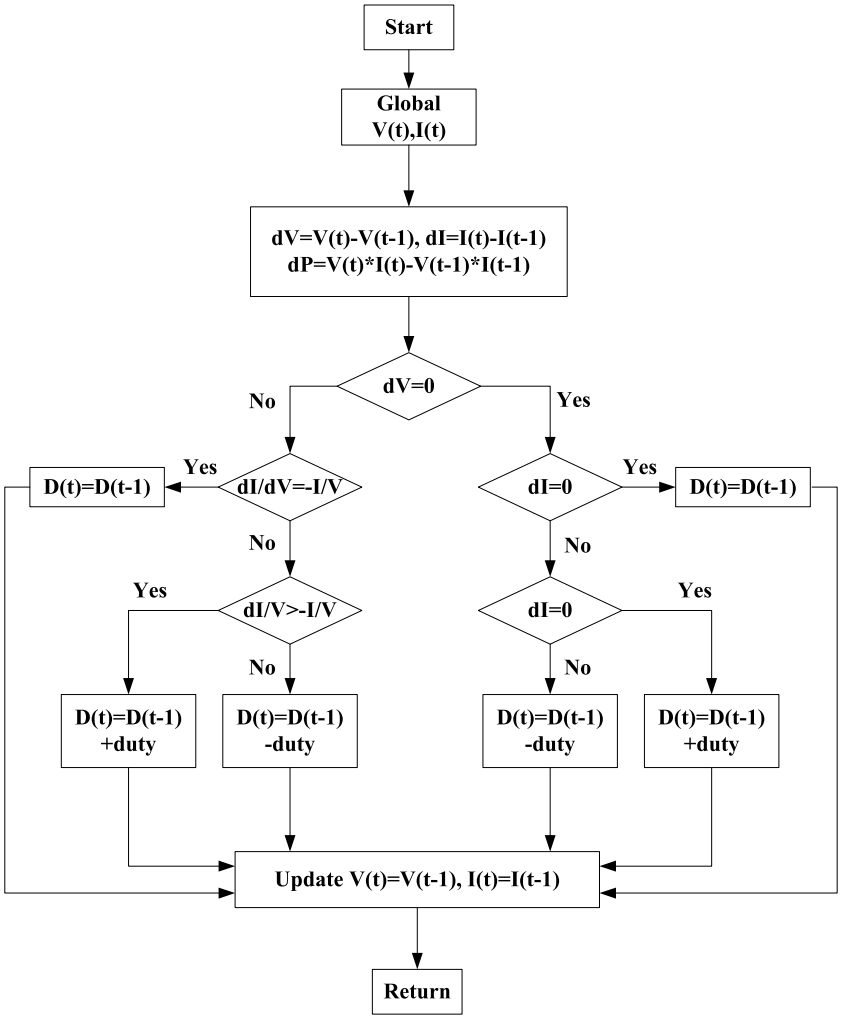

Fig. 3. Flow chart of Variable Step Size Incremental Conductance method.

In application, the MPPT Algorithm is connected between the solar cell and the DC/DC boost converter. The solar cell output controls the duty cycle of the power converter directly to reduce the complexity of system [13]. The flow chart of the improved MPPT algorithm of INC is shown in Fig. 3. The duty cycle of the converter is self-modulated.

In the system of output power of the solar cell directly controlling the duty cycle of the converter, $V(t)$ and $I(t)$ are the voltage and current of solar cell output in time t. $D(t)$ and duty are the duty cycle and the change of duty cycle. The design

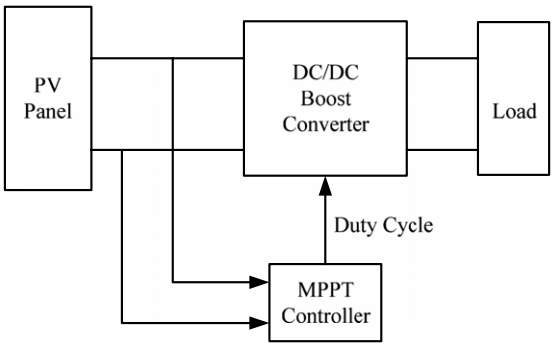

Fig. 4. MPPT control system of solar cell.

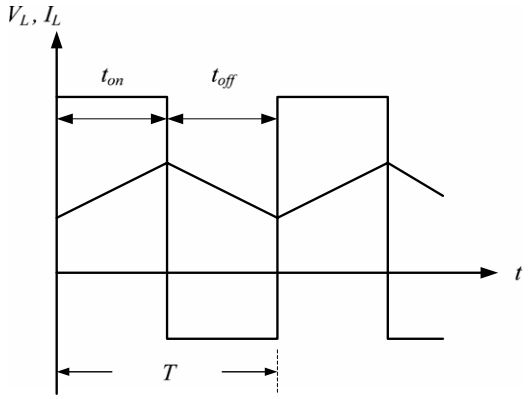

Fig. 5. Dynamical map of duty cycle of voltage and current.

of the variable step reduces the above problems, as shown in the following equation [14]

$$D(t) = D(t-1) \pm n \times |dP/dV| \tag{2}$$

where parameter n is the scaling factor for adjusting the step size.

The MPPT of PV can be realized by a DC/DC boost converter. The system is shown in Fig. 4. The MPPT controller is based on the Variable Step Size Incremental Conductance Method.

The operating principle of the DC/DC boost converter is shown in Fig. 5. The transistor cut-on time is t_{on}, and the transistor cut-off time is t_{off}. The operating mode of the DC/DC boost converter is shown in the figure. When $S_1 = 1$, it is in the cut-on state, the inductance voltage (V_L) equals the input voltage (V_{PV}). When $S_1 = 0$, it is in the cut-off state, the inductance voltage is the difference between input voltage and output voltage (V_o), t_{on} and t_{off} represent the cut-on and cut-off time cycles of the converter respectively. $T = t_{\text{on}} + t_{\text{off}}$. When the inductance ($L$) is in steady-state, the average voltage of one cycle is zero, the Eq. (1) can be obtained

$$\begin{aligned} 0 &= \int_{\text{on}} V_{\text{PV}} dt + \int_{\text{off}} (V_{\text{PV}} - V_o) dt \\ V_{\text{PV}} t_{\text{on}} &+ (V_{\text{PV}} - V_o) t_{\text{off}} = 0. \end{aligned} \tag{3}$$

According to Eq. (1)

$$\frac{V_o}{V_{\text{PV}}} = \frac{t_{\text{on}} + t_{\text{off}}}{t_{\text{off}}} = \frac{1}{1-D} \tag{4}$$

where $D = \frac{t_{om}}{T}$ is the switch duty cycle.

Fig. 6 shows the equivalent circuit of DC/DC boost converter in cut-on and cut-off. The mathematical equation of the voltage and current of the converter in different states can be deduced from this system.

When the transistor is in cut-off, i.e. $S = 0$, the mathematical equations of output voltage and current can be expressed as

$$\begin{aligned} \dot{i}_{L\cdot\text{off}} &= \frac{V_{\text{PV}}}{L} - \frac{V_o}{L} \\ \dot{V}_{o\cdot\text{off}} &= \frac{i_L}{C} - \frac{V_o}{CR_L}. \end{aligned} \tag{5}$$

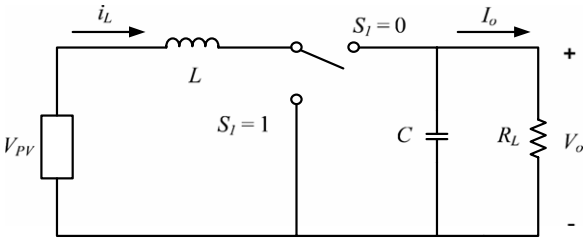

Fig. 6. DC/DC boost converter.

When the transistor is in cut-on, i.e. $S = 1$, the mathematical equation of output voltage and current can be expressed as

$$\dot{i}_{L\cdot\text{on}} = \frac{V_{\text{PV}}}{L}. \tag{6}$$

The dynamic equations can be deduced from Eqs. (3) and (4) by using the state space average method [15], and the duty cycle of transistor PWM is led in Eq. (5).

$$\dot{X} = (1 - D)\dot{X}_1 + D\dot{X}_2 \tag{7}$$

where $\dot{X}_1 = [\dot{i}_{L\cdot\text{off}}\dot{V}_{o\cdot\text{off}}]^T$, $\dot{X}_2 = [\dot{i}_{L\cdot\text{on}}\dot{V}_{o\cdot\text{on}}]^T$, duty cycle $D \in [0\ 1]$. Therefore, the dynamic equations can be deduced as follows

$$\begin{aligned}
\dot{i}_L &= (1 - D)\left(\frac{V_{\text{PV}}}{L} - \frac{V_o}{L}\right) + D\frac{V_{\text{PV}}}{L} \\
&= \frac{V_{\text{PV}}}{L} - \frac{V_o}{L} - D\frac{V_{\text{PV}}}{L} + D\frac{V_o}{L} + D\frac{V_{\text{PV}}}{L} \\
&= \frac{V_{\text{PV}}}{L} - \frac{V_o}{L} + D\frac{V_o}{L}
\end{aligned} \tag{8}$$

$$\begin{aligned}
\dot{V}_o &= (1 - D)\left(\frac{i_L}{C} - \frac{V_o}{CR_L}\right) + D\left(-\frac{V_o}{CR_L}\right) \\
&= \frac{i_L}{C} - \frac{V_o}{CR_L} - D\frac{i_L}{C} + D\frac{V_o}{CR_L} - D\frac{V_o}{CR_L} \\
&= \frac{i_L}{C} - \frac{V_o}{CR_L} - D\frac{i_L}{C}
\end{aligned} \tag{9}$$

where the duty cycle (D) represents the control input of the transistor. The inductance and resistance are neglected. If i_L is the solar cell current, the above equations can realize a nonlinear time varying system as follows

$$\dot{X} = f(X) + h(X)D \tag{10}$$

where $\dot{X} = [i_L V_o]^T$, $f(X) = [\frac{V_{\text{PV}}}{L} - \frac{V_O}{L}\frac{i_L}{C} - \frac{V_O}{CR_L}]$, $h(X) = [\frac{V_O}{L} - \frac{i_L}{C}]$.

4. Genetic algorithm

The Genetic Algorithm (GA) was first proposed by John Holland in 1960, who established the foundation of this algorithm in his *Adaptation in Natural and Artificial Systems* in 1975. The GA is one of optimization methods [16], which has fewer restrains on solving, does not require complicated and precise mathematical equations, and uses only the fitness function to search for a global optimal solution. The seven elements of the GA are:

- Defined chromosome condition.
- Generate initial population.
- Fitness function design.
- Selection.
- Crossover.
- Mutation.
- Termination condition.

The basic flow of the GA is shown in Fig. 7:

The determination of fitness function is the key point of the GA. The fitness function is the basis of searching for an optimal solution, i.e. identifying the adaptability of a chromosome, so as to decide the existence of a chromosome. In the search process of the GA, each generation produces an adaptive population. When this population is higher than the last generation, it means that the new population is better than the last generation's population, and the new generation's

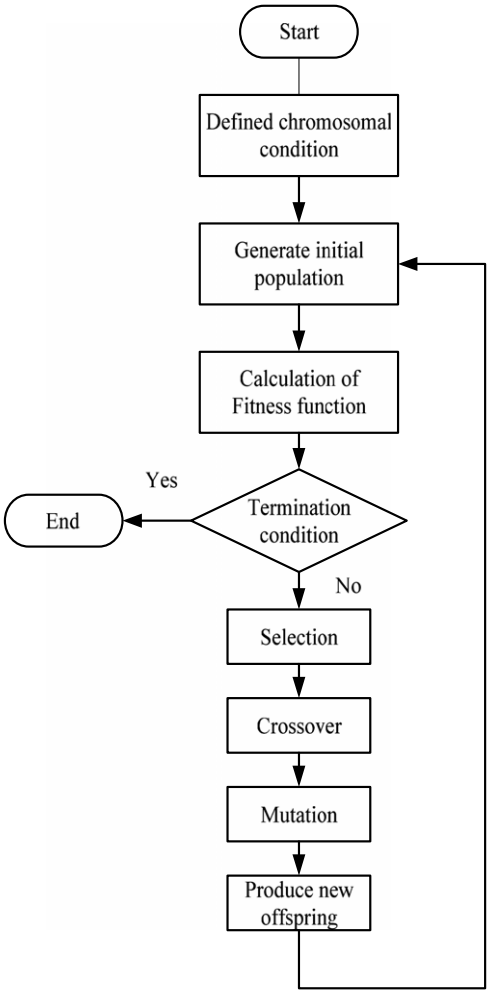

Fig. 7. Flow chart of GA.

excellent population is more likely to be preserved. Finally, the preserved population is the optimal solution of the fitness function. Therefore, the design quality of the fitness function will influence whether the GA can obtain an optimal solution.

The fitness function in this paper is designed as the absolute value and integral of errors between input and output, and the maximum value of each calculation process is taken as the adaptive value. This fitness function is expressed as follows

$$\text{IAE} = \int_0^\infty |e(t)|\, dt. \tag{11}$$

The rank of the GA is the calculation method. The adaptive values searched for in the out of calculation process are arranged in order.

5. Principle of battery charging

The CV is the mostly used method for the moment, charging the battery at a fixed voltage. It has a simple circuit architecture, and the control circuit is easy to design. The factor of voltage difference impels the battery to make a reverse chemical reaction to store energy. Fig. 8 shows the charging curve of CV.

The CV of this study uses a DC/DC buck converter that is connected to first-order output, so the voltage and current of first-order MPP controls the CV for Li-ion battery. The constant voltage structure is that the feedback output voltage uses a PI controller to control the duty cycle. As the PI controller can suppress high frequency noise to improve the system or to eliminate steady-state error, the battery output reaches a stable CV [17].

The second-order batter-charging system is shown in Fig. 9. The first-order output voltage controls the charging of the Li-ion battery via the buck converter, and the voltage feedback control of the Li-ion battery forms a closed-loop control system. This control system controls the battery charging voltage at $V_B \leq V_r$, so that the Li-ion battery is not over charged.

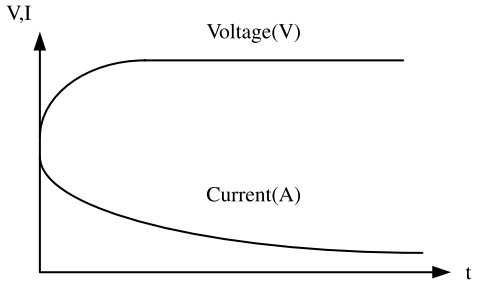

Fig. 8. Charging curve of CV.

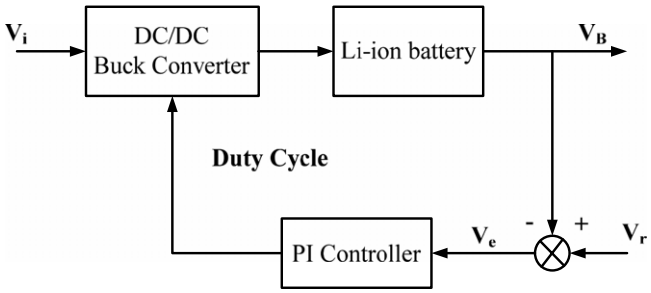

Fig. 9. Schematic diagram of charging control.

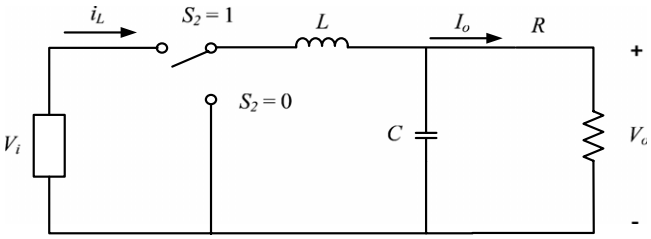

Fig. 10. DC/DC buck converter (simulated battery load).

The V_B is battery voltage, V_r is control voltage, V_e is the steady-state error of system. The steady-state error V_e is controlled to make

$$V_e = V_r - V_B. \tag{12}$$

The PI controller controls the steady-state error V_e at 0, so that the battery voltage V_B does not exceed control voltage V_r, thus achieving CV.

The operating principle of the DC/DC buck converter is the same as that of the boost converter, when $S_2 = 1$, it is in cut-on state, when $S_2 = 0$, it is in the cut-off state.

Fig. 10 shows the equivalent circuit of the DC/DC buck converter in cut-on and cut-off, the transfer function of input and output is deduced from this system

$$\begin{aligned} \frac{V_o}{V_i} &= U \times \frac{R(sCR+1)}{s^2RLC + sL + R} \\ &= U \times \frac{\frac{R}{L}s + \frac{1}{LC}}{s^2 + \frac{1}{RC}s + \frac{1}{LC}} \end{aligned} \tag{13}$$

where U is the duty cycle of the DC/DC Buck Converter.

The transfer function $T(s)$ of the whole charging system is deduced from the transfer function of the DC/DC Buck Converter and PI controller

$$\begin{aligned} T(s) &= \frac{V_o}{U} \times PI(s) \\ &= V_i \times \frac{\frac{R}{L}s + \frac{1}{LC}}{s^2 + \frac{1}{RC}s + \frac{1}{LC}} \times \frac{k_P s + k_I}{s}. \end{aligned} \tag{14}$$

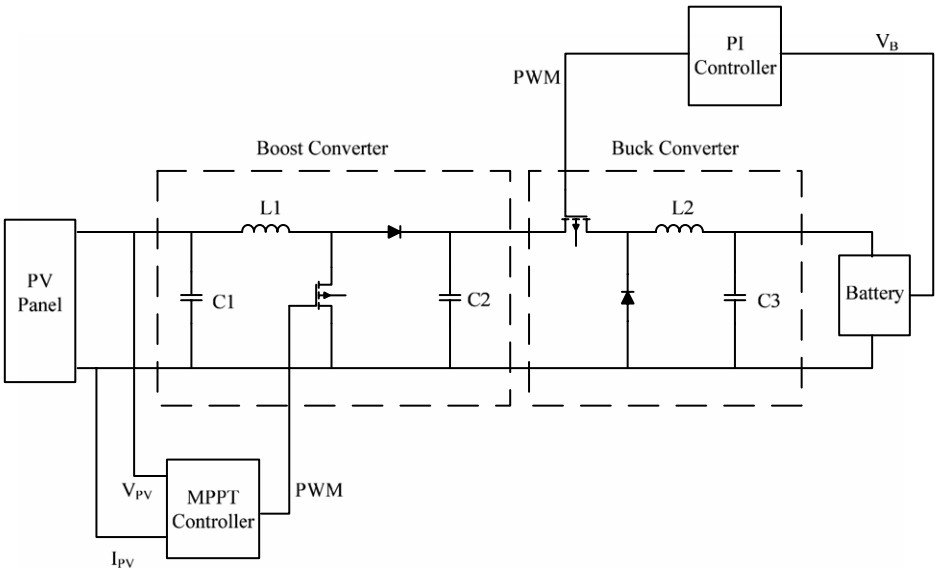

Fig. 11. System structure.

Table 1
Datasheet of SM8656.

P_{max}	V_{MPP}	I_{MPP}	V_{oc}	I_{sc}
0.25 W	2.5 V	100 mA	3 V	120 mA

This transfer function $T(s)$ is substituted in the RLC parameter value of this system to obtain

$$T(s) = 5 \times \frac{1.25 \times 10^6 s + 5 \times 10^7}{s^2 + 40s + 5 \times 10^7} \times \frac{k_P s + k_I}{s}. \tag{15}$$

This system is a closed loop transfer function. The characteristic equation of this function is determined using Routh table

$$A(s) = s^3 + [1.25 \times 10^6 k_P]s^2 + [5 \times 10^7 (k_P + 1) + 1.25 \times 10^6 k_I]s + 5 \times 10^7 k_I. \tag{16}$$

The result shows that if k_P and k_I are greater than 0, the poles of this system are in the left half of Plane s, namely, the stability of this system can be controlled when the PI controller is added in.

Fig. 11 shows the system structure of this paper. The PV Panel is the simulated solar cell. The MPPT controller generates the PWM of the duty cycle to drive the MosFET of the DC/DC boost converter, so that the solar cell works at the MPPT, and the cell terminal feeds back the voltage. The PI controller generates the PWM of the duty cycle to drive the MosFET of DC/DC Buck Converter

6. Simulation results

This study used SIMULINK and SIMPOWER of MATLAB to simulate solar panel of SM8656. The DATASHEET is shown in Table 1.

This study integrated solar MPPT with charging control of the Li-ion battery, and used the SIMULINK and SIMPOWER of MATLAB for simulation. The GAtool was used to realize the GA. The simulation results are shown below. The Li-ion battery in this study was a rechargeable Li-ion battery of BT-14 500-12 (3.7 V/1200 mAH). When the rechargeable Li-ion battery was fully charged, the voltage was about 4.2 V, and the battery may explode if the charging voltage exceeds 4.3 V.

Fig. 12 is the IAE convergence map of the GA. This algorithm uses the fitness function proposed by this study to search for the optimal solution of 0.1437 effectively. The PI parameter value searched by the GA is $[K_P K_I] = [0.4253\ 0.0623]$, which is the output power of the solar cell. Fig. 13 shows that the INC can track the MPPT of SM8656 rapidly, and the steady-state oscillation is small.

The constant voltage charging state of solar MPPT is shown in Figs. 13 and 14. Fig. 13 shows the maximum power in standard test conditions (i.e. 1000 W/m^2 solar irradiance, AM1.5, 25°). According to the simulation results, the MPPT can be tracked rapidly using the Variable Step Size Incremental Conductance Method, and the oscillation effect is very small in the steady-state. Fig. 14 shows that the PI feedback controlled CV can realize the voltage-stabilized charging of the charging system.

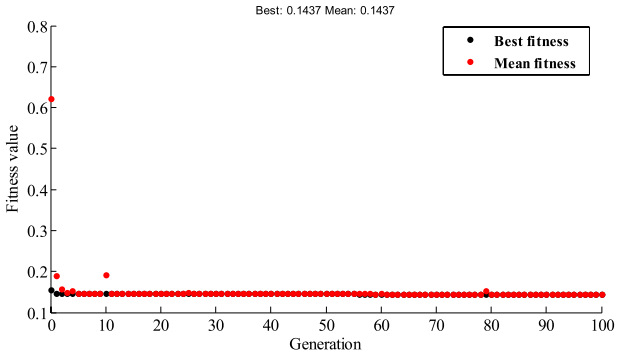

Fig. 12. IAE convergence map of GA.

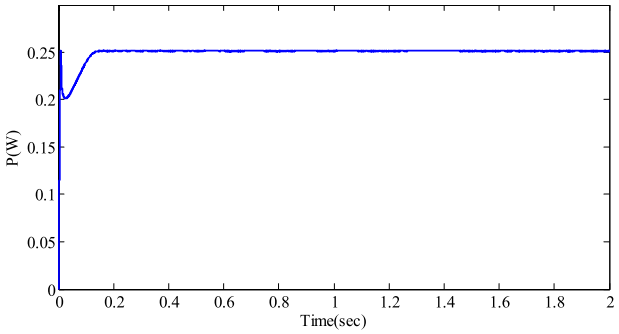

Fig. 13. Output power of solar cell.

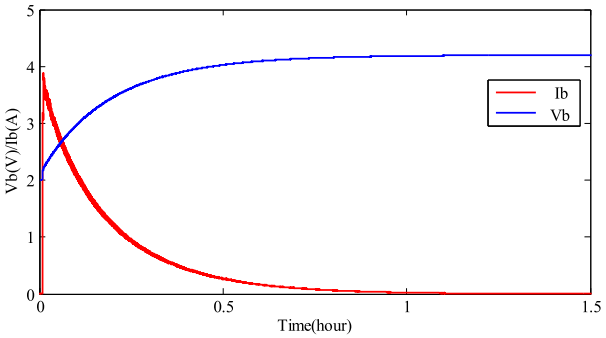

Fig. 14. Charging voltage and current of Li-ion battery.

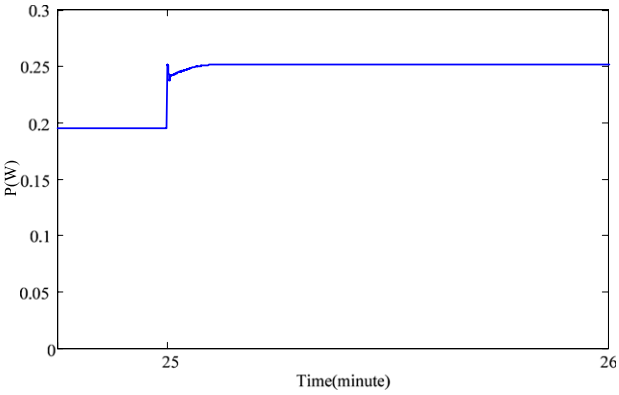

Fig. 15. Output power of solar cell when solar irradiance is changed (solar irradiance increased from 800 w/m^2 to 1000 w/m^2 at 25 min).

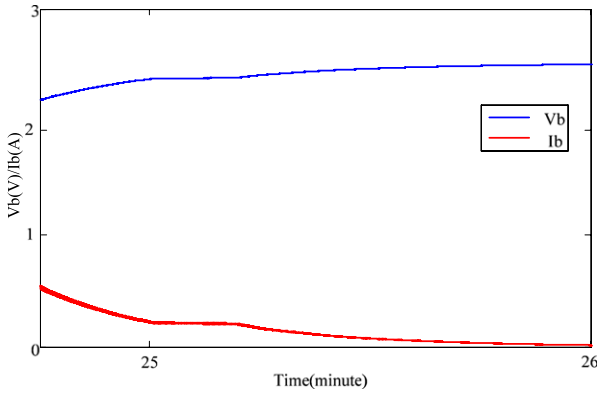

Fig. 16. Charging current and voltage of Li-ion battery when solar irradiance increased from 800 w/m^2 to 1000 w/m^2 at 25 min.

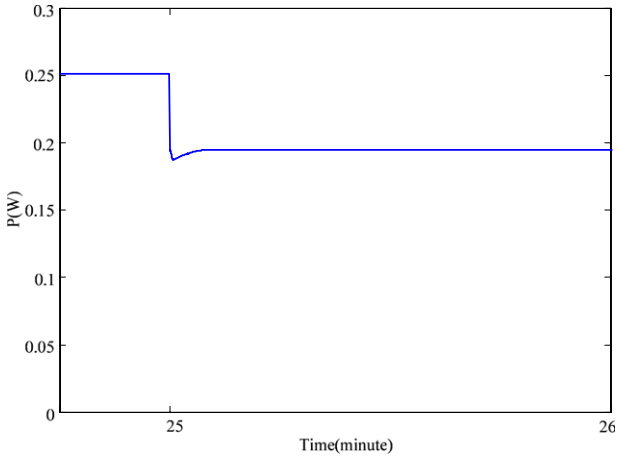

Fig. 17. Output power of solar cell when solar irradiance increased from 1000 w/m^2 to 800 w/m^2 at 25 min.

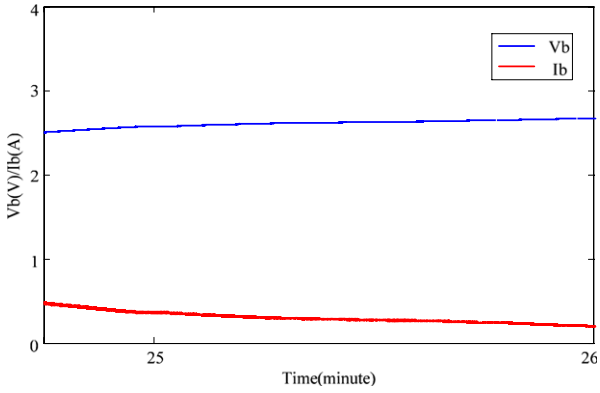

Fig. 18. Charging current and voltage of Li-ion battery when solar irradiance increased from 1000 w/m^2 to 800 w/m^2 at 25 min.

The simulation results of different solar irradiance conditions are shown in Figs. 15–18. Figs. 15 and 17 shows that the MPPT system used in this study can track the MPPT effectively by changing the solar irradiance conditions. Fig. 15 shows the MPPT when the solar irradiance increased from 800 w/m^2 to 1000 w/m^2 at 25 min. Fig. 17 shows the MPPT when the solar irradiance increased from 1000 w/m^2 to 800 w/m^2 at 25 min. Figs. 16 and 18 show the simulation results of changing the solar irradiance conditions. When the solar irradiance increased from 800 w/m^2 to 1000 w/m^2, the CV responded slowly and kept tracking 4.2 V charging. When the solar irradiance increased from 1000 w/m^2 to 800 w/m^2, it kept tracking 4.2 V charging rapidly. The results showed that the feedback PI controlled CV can charge the Li-ion battery effectively under any solar irradiance conditions.

7. Conclusions

Many previous studies focused on specific system control, whereas the PV charging system proposed by this study integrated the solar MPPT and developed the most efficient charging equipment for the Li-ion battery. This integrated system can utilize solar energy and control the charging of battery at maximum efficiency, so that the Li-ion battery can be fully charged within a short time. This system is thus proven to be feasible.

Moreover, this study used the simplest CV to minimize the cost. The simulation results for different solar irradiance conditions showed that this system can track the MPPT under any condition, and the charging system can charge the Li-ion battery efficiently. The integrated system can be applied to portable equipments in the future to realize small and low cost solar chargers.

Acknowledgments

The financial support of this research by the National Science Council of the R.O.C., under Grant No. NSC 100-2628-E-167-002-MY3 and NSC 100-2622-E-167-005-CC3 is greatly appreciated.

References

[1] G. de Cesare, D. Caputo, A. Nascetti, Maximum power point tracker for portable photovoltaic systems with resistive-like load, Sol. Energy 80 (8) (2006) 982–988.
[2] R. Kadri, J.P. Gaubert, G. Champenois, An improved maximum power point tracking for photovoltaic grid-connected inverter based on photovoltaic grid-connected inverter, IEEE Trans. Ind. Electron. 58 (1) (2011) 66–75.
[3] L. Zhang, A.A. Amoudi, Y.F. Bai, Real-Time Maximum Power Point Tracking for Grid-Connected Photovoltaic System (Proceedings of the 8th International Conference on Power Electronics and Variable Speed Drives), 2000, pp. 124–129.
[4] A. Safari, S. Mekhilef, Simulation and hardware implementation of incremental conductance MPPT with direct control method using cuk converter, IEEE Trans. Ind. Electron. 58 (4) (2011) 1154–1161.
[5] Q. Mei, M. Shan, L. Liu, J.M. Guerrero, A novel improved variable step-size incremental-resistance MPPT method for PV systems, IEEE Trans. Ind. Electron. 58 (6) (2011) 2427–2434.
[6] W.J. Sohn, T.J. Chainer, Constant-current versus constant-voltage VCM drive analysis, IEEE Trans. Magn. 26 (3) (1990) 1217–1224.
[7] M. Chen, G.A. Rincón-Mora, Accurate, compact, and power-efficient Li-ion battery charger circuit, IEEE Trans. Circuits Syst. Express Briefs 53 (11) (2006) 1180–1184.
[8] B.Y. Chen, Y.S. Lai, New digital-controlled technique for battery charger with constant current and voltage control without current feedback, IEEE Trans. Ind. Electron. 59 (3) (2012) 1545–1553.
[9] Y.X. Zhou, B.L. Zhang, D. Bu, N.H. Wang, Y.N. Wang, X.D. Liang, Z.C. Guan, Nanosecond pulse corona charging of polymers, IEEE Trans. Dielectr. Electr. Insul. 14 (2) (2007) 495–501.
[10] L.R. Chen, N.Y. Chu, C.S. Wang, R.H. Liang, Design of a reflex-based bidirectional converter with the energy recovery function, IEEE Trans. Ind. Electron. 55 (8) (2008) 3022–3029.
[11] D.D. Lu, V.G. Agelidis, Photovoltaic-battery-powered DC bus system for common portable electronic devices, IEEE Trans. Power Electron. 24 (3) (2009) 849–855.
[12] F. Liu, S. Duan, F. Liu, B. Liu, Y. Kang, A variable step size INC MPPT method for PV systems, IEEE Trans. Ind. Electron. 55 (7) (2008) 2622–2628.
[13] N. Femia, D. Granozio, G. Petrone, G. Spagnuolo, M. Vitelli, Predictive & adaptive MPPT perturb and observe method, IEEE Trans. Aerosp. Electron. Syst. 43 (3) (2007) 934–950.
[14] A. Pandey, N. Dasgupta, A.K. Mukerjee, Design issues in implementing MPPT for improved tracking and dynamic performance, in: Proceeding of the 32nd Annual Conference of the IEEE Industrial Electronics, 2006, pp. 4387–4391.
[15] C.C. Chu, C.L. Chen, Robust maximum power point tracking method for photovoltaic cells: a sliding mode control approach, Sol. Energy 83 (2009) 1370–1378.
[16] A.H. Mantawy, Y.L. Abdel-Magid, S.Z. Selim, INTEGRATING genetic algorithms, tabu search, and simulated annealing for the unit commitment problem, IEEE Trans. Power Syst. 14 (3) (1999) 829–836.
[17] K.M. Tsang, W.L. Chan, Current sensorless quick charger for lithium-ion batteries, Energy Convers. Manage. 52 (3) (2011) 1593–1595.